Biochemical Engineering Journal 121 (2017) 118–130

Contents lists available at ScienceDirect

Biochemical Engineering Journal

journal homepage: www.elsevier.com/locate/bej

Regular article

Three-phase fluidized bed bioreactor modelling and simulation

Szymon Skoneczny*, Wojciech Stryjewski, Katarzyna Bizon, Bolesław Tabiś

Department of Chemical and Process Engineering, Cracow University of Technology, Poland

ARTICLE INFO

Article history:
Received 14 March 2016
Received in revised form 19 October 2016
Accepted 28 January 2017
Available online 31 January 2017

Keywords:
Fluidized bed
Bioreactor
Mathematical modelling
Steady states
Stability
Oscillations

ABSTRACT

A mathematical model of a three-phase fluidized bed biofilm reactor for aerobic processeses is presented. The growth of attached biomass, its decay and interphase transfer were taken into consideration in the proposed quantitative description of the bioreactor. The presented model of the fluidized-bed bioreactor is the unique one which takes into account partial thickening of biomass and its recirculation. The stationary characteristics was determined with the use of a novel simplified numerical method for the assessment of stability of steady states. The effect of microbial growth kinetics on steady state multiplicity was characterized. The relationship between biofilm growth and boundaries of fluidized bed existence was shown. Conditions of the biofilm's existence on carrier particles were formulated. Some novel dynamic characteristics concerning fluidized bed bioreactors were presented.

1. Introduction

Three-phase fluidized bed biofilm reactors are commonly used in environmental protection engineering and biotechnology. Among other uses, they are used to carry out microbiological degradation processes of toxic organic compounds [1–5], microbiological nitrification process [6] and synthesis of some drugs, e.g. penicillin, oxytetracycline and other organic compounds [7–9], and in the production of yeast [10]. A review of numerous applications of three-phase fluidized bed bioreactors was presented by Schügerl [11].

The key advantages of fluidized bed bioreactors are: highly expanded interphase surface, simple construction and, above all, the possibility of the separation of the mean residence time of the liquid phase and the immobilized biomass. Moreover, immobilization of biomass on fine particles results in a many times higher concentration of biomass in comparison with stirred tank bioreactors with suspended cells. According to Tang and Fan [2], due to the immobilization of the microorganisms the concentration of biomass in a fluidized bed reactor can be up to 30–40 kg/m^3, i.e. around ten times higher than in tank bioreactors with activated sludge. As arises from unstructured kinetics, rates of microbiological processes is proportional to the concentration of active biomass in the reaction environment. The application of fluidized bed bioreactors also eliminates the phenomenon of bed clogging, which is commonly observed in biofilters with a fixed bed.

In view of the numerous applications of three-phase fluidized bed bioreactors in biotechnology, research focused on the mathematical modelling and simulation of these apparatuses has been in progress for many years. Heterogeneous models for aerobic microbiological processes were published in the 1980s. Representative works from this period are papers by Park, Davis and Wallis [7,8], Chang and Rittmann [12], Tang et al. [2,3], Worden and Donaldson [5], and Wisecarver and Fan [4].

In the early 2000 s Onysko et al. [1] applied an integral approximation method for the modelling of biofilm dynamics in a study concerning the dynamics of a fluidized bed bioreactor. The authors analysed a process with a single limiting substrate. The first works concerning the application of nonlinear analysis for the investigation of the stationary and dynamic properties of three-phase fluidized bed bioreactors were published in the first decade of the 21st century [13].

The most recent mathematical model of the three-phase fluidized bed bioreactor has been proposed by Olivieri et al. [14]. However, the model assumes a lack of mass transfer resistance between the liquid phase and the biofilm, and the decay of immobilized biomass is also omitted. Moreover, the cited authors did not take into account the distributions of diffusion coefficients and biomass density in the biofilm. Hence, a more general model has been proposed, and furthermore, an analysis of the influence of several process parameters which have not been taken into account in the literature has been conducted.

* Corresponding author at: Department of Chemical and Process Engineering, Cracow University of Technology, ul. Warszawska 24, 31-155 Cracow, Poland.
E-mail address: skoneczny@chemia.pk.edu.pl (S. Skoneczny).

http://dx.doi.org/10.1016/j.bej.2017.01.017
1369-703X/

Nomenclature

a_s	Specific external biofilm surface area (m^{-1})
ak_c	Gas-liquid volumetric mass transfer coefficient (h^{-1})
Bi $_i$	Biot number, (i = A, T)
c_A, c_B, c_T	Mass concentration of carbonaceous substrate, biomass and oxygen, respectively ($kg\,m^{-3}$)
d_0	Diameter of a solid carrier (m)
D_e	Effective diffusion coefficient in biofilm ($m^2\,h^{-1}$)
F_V	Volumetric flow rate ($m^3\,h^{-1}$)
h	Height coordinate in the apparatus (m)
H	Total height of the fluidized bed (m)
k	Maximum specific growth rate (h^{-1})
k_o	Decay rate coefficient(h^{-1})
k_{det}	Biofilm detachment rate coefficient (h^{-1})
k_s	Liquid-biofilm mass transfer coefficient ($m\,h{-}1$)
K_A, K_T	Saturation constants for carbonaceous substrate and oxygen in kinetic equations ($kg\,m^{-3}$)
K	Gas-liquid interphase equilibrium constant
K_{in}	Inhibition constant ($kg\,m^{-3}$)
L_b	Thickness of the biofilm (m)
m_B	Total mass of biomass (kg)
n_s	Number of carrier particles
N	Number of internal collocation points
r_A, r_T	Uptake rate of carbonaceous substrate and oxygen, respectively ($kg\,m^{-3}\,h^{-1}$)
r_B	Growth rate of biomass ($kg\,m{-}^3\,h{-}^1$)
r_b	Radius of the bioparticle (m)
r_{det}	Detachment rate of biomass ($kg\,m^{-3}\,h^{-1}$)
r_0	Radius of the carrier particle (m)
S	Cross-sectional area of the apparatus (m^2)
t	Time (h)
u	Superficial velocity ($m\,s{-}1$)
u_b	Bubble rise velocity ($m\,s{-}^1$)
u_{0g}	Superficial air velocity ($m\,s{-}^1$)
V	Volume (m^3)
w_{BA}, w_{BT}	Yield coefficients (kg B·kg A^{-1}), (kg B·kg T^{-1})
x	Current coordinate in the biofilm (m)
x_a	Fraction of active biomass in the biofilm
z	Dimensionless coordinate in the biofilm
Z	Dimensionless coordinate in the fluidized bed
α	Degree of conversion of the carbonaceous substrate
β	Dimensionless concentration of biomass in liquid phase
γ	Dimensionless concentration of oxygen in liquid phase
δ	Dimensionless concentration of oxygen in the biofilm
ε_g	Gas hold-up in the multi-phase system
ζ	Fraction of carrier particles in the liquid
η	Dimensionless concentration of carbonaceous substrate in the biofilm
ϑ	Biomass thickening coefficient
ξ	Recirculation ratio of the liquid
ρ_a	Concentration of active biomass in the biofilm ($kg\,m^{-3}$)
ρ_b	Concentration of biomass in the biofilm ($kg\,m^{-3}$)
$\bar{\rho}_b$	Average concentration of biomass in the biofilm ($kg\,m^{-3}$)
ρ_0	Density of solid carrier ($kg\,m^{-3}$)
τ_0^c	Mean residence time of the liquid in the installation (h)
Φ	Thiele modulus

Nomenclature

Superscripts

b	Biofilm phase
c	Liquid (continuous) phase
g	Gas phase

Subscripts

A, B, T	Refer to carbonaceous substrate, biomass and oxygen, respectively
s	Refers to surface of the biofilm
f	Refers to feed stream
r	Refers to recirculated stream

A comparison of the proposed mathematical model with other models of a three-phase fluidized bed bioreactor for aerobic processes is presented in Table 1. It can be seen from Table 1 that the presented model is the unique one which takes into account the partial thickening of biomass and its recirculation. Apart from this, a novel simplified numerical method for the assessment of stability of steady states was proposed, which is based on hypothesis concerning concentration distributions in the biofilm and its surroundings. The proposed model was used for the nonlinear analysis of the steady states, and for the analysis of the dynamic behaviour of the three-phase fluidized bed bioreactor with double-substrate limited processes.

2. Mathematical model of the bioreactor

The mathematical model of the fluidized bed bioreactor consists of: a quantitative description of fluidized bed hydrodynamics, interphase mass transfer, kinetics of the microbiological process, and dynamics of biofilm growth on fine carrier particles (Fig. 1).

A schematic diagram of the analysed bioreactor is presented in Fig. 2. Symbols used in the mathematical model of the installation have been marked in this figure.

2.1. Model of a microbiological process in biofilm

Beyenal and Tanyolac [16] proved experimentally that the standard deviation of the mean biofilm thickness is sufficiently small to use a mean value in calculations. This assumption is applied in this work. A representative volume in the biofilm is a sphere with a differential thickness. In mass balance equations formulated for the representative volume, the following terms are taken into account:

a) diffusional mass inflow and outflow,
b) utilization of substrates due to the microbiological process,
c) accumulation of substrates.

The application of the mass conservation principle for the carbonaceous substrate A and oxygen T gives the following equations

$$4\pi x^2 \frac{\partial c_A^b}{\partial t} dx = 4\pi x^2 D_{eA} \frac{\partial c_A^b}{\partial x} - 4\pi(x-dx)^2 \cdot \left(D_{eA} \cdot \frac{\partial c_A^b}{\partial x} - \frac{\partial}{\partial x} D_{eA} \frac{\partial c_A^b}{\partial x} dx \right) - 4\pi x^2 \cdot r_A^b(c_A^b, c_T^b, x)\,dx \quad (1a)$$

$$4\pi x^2 \frac{\partial c_T^b}{\partial t} dx = 4\pi x^2 D_{eT} \frac{\partial c_T^b}{\partial x} - -4\pi(x-dx)^2 \cdot \left(D_{eT} \cdot \frac{\partial c_T^b}{\partial x} - \frac{\partial}{\partial x} D_{eT} \frac{\partial c_T^b}{\partial x} dx \right) - 4\pi x^2 \cdot r_T^b(c_A^b, c_T^b, x)\,dx \quad (1b)$$

Table 1
Comparison of models for a three-phase fluidized-bed bioreactor for aerobic processes.

	Reference							
Assumption	This study	[7]	[2]	[3]	[15]	[1]	[4]	[14]
Double-substrate growth kinetics	●	●	●	●	●	○	●	●
Distribution of biomass density in the biofilm	●	○	○	●	○	○	○	○
Distributions of diffusion coefficients in the biofilm	●	○	○	○	○	○	●	○
Microbiological process in the liquid phase	●	○	○	○	○	●	○	●
External mass transfer resistances	●	○	●	●	●	●	●	○
Biofilm detachment	●	○	○	●	○	●	○	●
Gas-liquid mass transfer	●	○	●	●	○	○	●	●
Biomass decay in the biofilm	●	○	○	●	○	○	○	○
Partial recirculation of the biomass and its thickening	●	○	○	○	○	○	○	○
Topic	This study	[7]	[2]	[3]	[15]	[1]	[4]	[14]
Determination of steady state branches	●	○	●	○	○	○	●	●
Dynamic analysis	●	●	○	●	●	●	○	●
Stability determination	●	○	○	○	○	○	○	●

○ assumption not made/topic not realized; ● assumption made/topic realized.

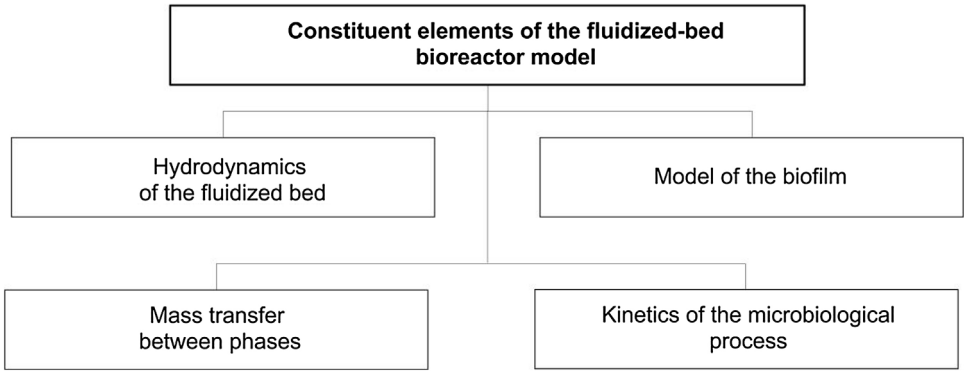

Fig. 1. Constituent elements of the mathematical model of the fluidized bed bioreactor.

After performing mathematical operations, which result from the form of Eqs. (1) and applying Weierstrass's theorem about the limitation of a continuous function on compact sets, one obtains

$$\frac{\partial c_A^b}{\partial t} = \frac{1}{x^2}\frac{\partial}{\partial x}\left(x^2 D_{eA}(x)\frac{\partial c_A^b}{\partial x}\right) - r_A^b(c_A^b, c_T^b, x) \quad (2a)$$

$$\frac{\partial c_T^b}{\partial t} = \frac{1}{x^2}\frac{\partial}{\partial x}\left(x^2 D_{eT}(x)\frac{\partial c_T^b}{\partial x}\right) - r_T^b(c_A^b, c_T^b, x) \quad (2b)$$

Eqs.(2) are subject to the following boundary and initial conditions (3)

$$\frac{\partial c_A^b(0,t)}{\partial x} = 0, \quad t \geq 0 \quad (3a)$$

$$\frac{\partial c_T^b(0,t)}{\partial x} = 0, \quad t \geq 0 \quad (3b)$$

$$D_{eA}\frac{\partial c_A^b(L_b,t)}{\partial x} = k_{sA}\left(c_A^c - c_{As}\right), \quad t \geq 0 \quad (3c)$$

$$D_{eT}\frac{\partial c_T^b(L_b,t)}{\partial x} = k_{sT}\left(c_T^c - c_{Ts}\right), \quad t \geq 0 \quad (3d)$$

$$c_A^b(x,0) = c_{0A}^b(x), \quad x \in [0, L_b] \quad (4a)$$

$$c_T^b(x,0) = c_{0T}^b(x), \quad x \in [0, L_b] \quad (4b)$$

Knowledge of effective diffusion coefficients D_{ei}, density ρ_b, biofilm thickness L_b and microbial growth kinetics is necessary to solve the boundary value problem describing the process in the biofilm. Double-substrate limited microbiological processes with Monod-Monod and Haldane-Monod kinetics are taken into account

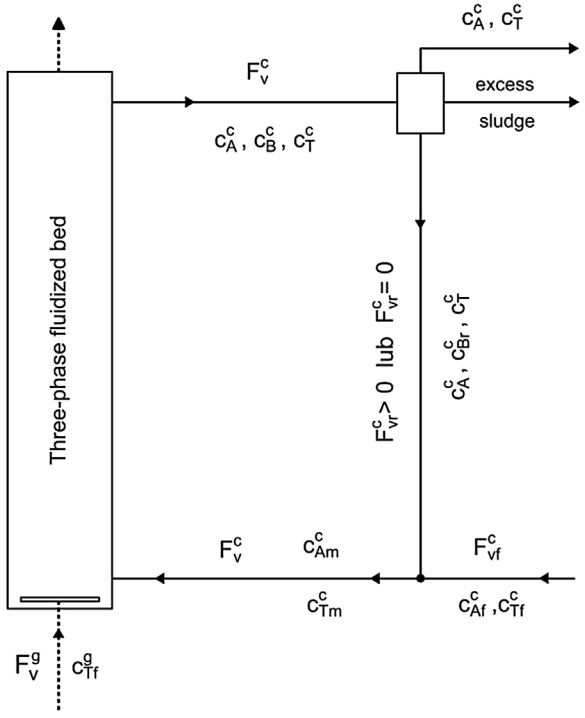

Fig. 2. Schematic diagram of the three-phase fluidized bed bioreactor with external recirculation.

in this work. Hence, the uptake rate of the carbonaceous substrate A and oxygen T in the biofilm can be formulated as follows

$$r_{\mathrm{A}}^{b}(c_{\mathrm{A}}^{b}, c_{\mathrm{T}}^{b}) = \frac{1}{w_{\mathrm{BA}}} \cdot f_1(c_{\mathrm{A}}^{b}) \cdot f_2(c_{\mathrm{T}}^{b})\, \rho_b x_a \tag{5a}$$

$$r_{\mathrm{T}}^{b}(c_{\mathrm{A}}^{b}, c_{\mathrm{T}}^{b}) = \frac{1}{w_{\mathrm{BT}}} \cdot f_1(c_{\mathrm{A}}^{b}) \cdot f_2(c_{\mathrm{T}}^{b})\, \rho_b x_a \tag{5b}$$

Functions $f_1(c_{\mathrm{A}}^{b})$ and $f_2(c_{\mathrm{T}}^{b})$ depend on the process type. For Monod-Monod kinetics they are defined as

$$f_1(c_{\mathrm{A}}^{b}) = \frac{k \cdot c_{\mathrm{A}}^{b}}{K_{\mathrm{A}} + c_{\mathrm{A}}^{b}}, \quad f_2(c_{\mathrm{T}}^{b}) = \frac{c_{\mathrm{T}}^{b}}{K_{\mathrm{T}} + c_{\mathrm{T}}^{b}} \tag{6}$$

For Haldane-Monod kinetics one obtains

$$f_1(c_{\mathrm{A}}^{b}) = \frac{k \cdot c_{\mathrm{A}}^{b}}{K_{\mathrm{A}} + c_{\mathrm{A}}^{b} + \frac{(c_{\mathrm{A}}^{b})^2}{K_{in}}}, \quad f_2(c_{\mathrm{T}}^{b}) = \frac{c_{\mathrm{T}}^{b}}{K_{\mathrm{T}} + c_{\mathrm{T}}^{b}} \tag{7}$$

Variations of the biofilm thickness over time and the influence of process conditions on this state variable can be determined when additional equation is formulated. This equation describes the global biomass balance in the biofilm. The thickness of biofilm is always finite, which stems from three coexisting factors, i.e. biomass growth in the biofilm, its decay, and its detachment. In this work it is assumed that the biomass detachment rate is proportional to the volume of the biofilm [3,14].

The equation of a global mass balance of the biofilm, i.e. of both active and inactive microbial cells, is related to the whole volume of biofilm and has the form

$$\frac{dm_{\mathrm{B}}^{b}}{dt} = V^{b} \bar{r}_{\mathrm{B}}^{b} - k_{\mathrm{det}}\, V^{b} \bar{\rho}_b \tag{8}$$

The average biomass growth rate in the biofilm $\bar{r}_{\mathrm{B}}^{b}$ is defined by the following expression

$$\bar{r}_{\mathrm{B}}^{b} = \frac{3}{r_b^3 - r_0^3} \cdot \int_{r_o}^{r_b} x^2 \cdot r_{\mathrm{B}}^{b}(c_{\mathrm{A}}^{b}, c_{\mathrm{T}}^{b}, x) dx \tag{9}$$

Eq. (8) can be transformed and reduced to the form describing the dynamics of the biofilm thickness. Hence, one obtains

$$\frac{dL_b}{dt} = \frac{1}{3\bar{\rho}_b} \frac{r_b^3 - r_0^3}{r_b^2} \cdot \bar{r}_{\mathrm{B}}^{b} - \frac{k_{\mathrm{det}}}{3} \cdot \frac{r_b^3 - r_0^3}{r_b^2} \tag{10}$$

with the initial condition

$$L_b(0) = L_{0b} \tag{11}$$

where

$$\bar{\rho}_b = \frac{3}{r_b^3 - r_0^3} \cdot \int_{r_o}^{r_b} x^2 \cdot \rho_b(x) dx \tag{12}$$

The mass balance of active microbial cells in the biofilm is necessary to determine their mass ratio in the biofilm. Then, besides biomass growth and transfer to the liquid phase, decay should also be taken into account. Hence, one obtains

$$\frac{d\left(m_{\mathrm{B}}^{b} \cdot x_a\right)}{dt} = V^{b} \bar{r}_{\mathrm{B}}^{b} - k_{\mathrm{det}} V^{b} \bar{\rho}_b x_a - k_o V^{b} \bar{\rho}_b x_a \tag{13}$$

At a steady state the time derivatives are equal to zero in Eq. (8) and Eq. (13). Hence, the right hand sides of above-mentioned equations can be equated, obtaining

$$x_a = \frac{k_{\mathrm{det}}}{k_{\mathrm{det}} + k_o} \tag{14}$$

2.2. Models for liquid and gas phases

Based on the mass balances of the carbonaceous substrate A, biomass B and dissolved oxygen T, Eqs. (15) are obtained

$$V^{c} \frac{dc_{\mathrm{A}}^{c}}{dt} = F_V^{c}\left(c_{\mathrm{A}m}^{c} - c_{\mathrm{A}}^{c}\right) - V^{c} \cdot r_{\mathrm{A}}^{c}(c_{\mathrm{A}}^{c}, c_{\mathrm{B}}^{c}, c_{\mathrm{T}}^{c}) - k_{s\mathrm{A}} A_s \left(c_{\mathrm{A}}^{c} - c_{\mathrm{A}s}\right) \tag{15a}$$

$$V^{c} \frac{dc_{\mathrm{B}}^{c}}{dt} = F_V^{c}\left(c_{\mathrm{B}m}^{c} - c_{\mathrm{B}}^{c}\right) + V^{c} \cdot r_{\mathrm{B}}^{c}(c_{\mathrm{A}}^{c}, c_{\mathrm{B}}^{c}, c_{\mathrm{T}}^{c}) + k_{\mathrm{det}} \cdot V^{b} \bar{\rho}_b x_a \tag{15b}$$

$$V^{c} \frac{dc_{\mathrm{T}}^{c}}{dt} = F_V^{c}\left(c_{\mathrm{T}m}^{c} - c_{\mathrm{T}}^{c}\right) - V^{c} \cdot r_{\mathrm{T}}^{c}(c_{\mathrm{A}}^{c}, c_{\mathrm{B}}^{c}, c_{\mathrm{T}}^{c}) - k_{s\mathrm{T}} A_s \left(c_{\mathrm{T}}^{c} - c_{\mathrm{T}s}\right) + \mathrm{V\,a} k_{c\mathrm{T}} \cdot \int_0^1 \left(\frac{c_{\mathrm{T}}^{g}(Z)}{K} - c_{\mathrm{T}}^{c}\right) dZ \tag{15c}$$

where $Z = \frac{h}{H} \in [0, 1]$ is the dimensionless height of the fluidized bed.

In Eqs. (15) the quantity A_s denotes the external surface of bioparticles, while the biofilm volume is denoted as V^b. These quantities were calculated according to the following formulas

$$A_s = a_s \cdot \left(V^{c} + V^{g} + V^{s}\right) = V^{c} \cdot \frac{a_s}{(1-\varepsilon_g)(1-\zeta)} \tag{16}$$

$$V^{b} = n_s \cdot \frac{4}{3}\pi \left(r_b^3 - r_0^3\right) = V^{c} \cdot \frac{\zeta}{1-\zeta}\left(\frac{r_b^3}{r_0^3} - 1\right) \tag{17}$$

The volumetric ratio of gas in the three-phase environment of the process ε_g, the volumetric ratio of inert particles in the liquid phase $\zeta$and the specific surface area of bioparticles a_s, i.e. carriers covered with the biofilm, are defined as follows

$$\varepsilon_g = \frac{V^{g}}{V^{c} + V^{g} + V^{s}}, \; \zeta = \frac{V^{s}}{V^{c} + V^{s}}, \; a_s = \frac{A_s}{V^{c} + V^{g} + V^{s}} \tag{18}$$

When Eqs. (18) are introduced to the model of the liquid phase (15) one obtains

$$V^{c} \frac{dc_{\mathrm{A}}^{c}}{dt} = F_V^{c}\left(c_{\mathrm{A}m}^{c} - c_{\mathrm{A}}^{c}\right) - V^{c} \cdot r_{\mathrm{A}}^{c}(c_{\mathrm{A}}^{c}, c_{\mathrm{B}}^{c}, c_{\mathrm{T}}^{c}) - V^{c} \frac{a_s}{(1-\varepsilon_g)(1-\zeta)} k_{s\mathrm{A}} \left(c_{\mathrm{A}}^{c} - c_{\mathrm{A}s}\right) \tag{19a}$$

$$V^{c} \frac{dc_{\mathrm{B}}^{c}}{dt} = F_V^{c}\left(c_{\mathrm{B}m}^{c} - c_{\mathrm{B}}^{c}\right) + V^{c} \cdot r_{\mathrm{B}}^{c}(c_{\mathrm{A}}^{c}, c_{\mathrm{B}}^{c}, c_{\mathrm{T}}^{c}) + V^{c} \frac{\zeta}{1-\zeta} k_{\mathrm{det}} \left(\frac{r_b^3}{r_0^3} - 1\right) \bar{\rho}_b x_a \tag{19b}$$

$$V^{c} \frac{dc_{\mathrm{T}}^{c}}{dt} = F_V^{c}\left(c_{\mathrm{T}m}^{c} - c_{\mathrm{T}}^{c}\right) - V^{c} \cdot r_{\mathrm{T}}^{c}(c_{\mathrm{A}}^{c}, c_{\mathrm{B}}^{c}, c_{\mathrm{T}}^{c}) - V^{c} \frac{a_s}{(1-\varepsilon_g)(1-\zeta)} k_{s\mathrm{T}} \left(c_{\mathrm{T}}^{c} - c_{\mathrm{T}s}\right) + V^{c} \frac{a k_{c\mathrm{T}}}{(1-\varepsilon_g)(1-\zeta)} \cdot \int_0^1 \left(\frac{c_{\mathrm{T}}^{g}(Z)}{K} - c_{\mathrm{T}}^{c}\right) dZ \tag{19c}$$

Eqs. (19) are subject to boundary conditions:

$$c_{\mathrm{A}}^{c}(0) = c_{\mathrm{A}0}^{c}, \; c_{\mathrm{B}}^{c}(0) = c_{\mathrm{B}0}^{c}, \; c_{\mathrm{T}}^{c}(0) = c_{\mathrm{T}0}^{c} \tag{20}$$

Kinetic equations in mass balances (19) have the forms:

$$r_{\mathrm{B}}^{c}(c_{\mathrm{A}}^{c}, c_{\mathrm{B}}^{c}, c_{\mathrm{T}}^{c}) = f_1(c_{\mathrm{A}}^{c}) \cdot f_2(c_{\mathrm{T}}^{c})\, c_{\mathrm{B}}^{c} \tag{21a}$$

$$r_{\mathrm{A}}^{c}(c_{\mathrm{A}}^{c}, c_{\mathrm{B}}^{c}, c_{\mathrm{T}}^{c}) = \frac{1}{w_{\mathrm{BA}}} \cdot r_{\mathrm{B}}^{c}(c_{\mathrm{A}}^{c}, c_{\mathrm{B}}^{c}, c_{\mathrm{T}}^{c}) \tag{21b}$$

$$r_{\mathrm{T}}^{c}(c_{\mathrm{A}}^{c}, c_{\mathrm{B}}^{c}, c_{\mathrm{T}}^{c}) = \frac{1}{w_{\mathrm{BT}}} \cdot r_{\mathrm{B}}^{c}(c_{\mathrm{A}}^{c}, c_{\mathrm{B}}^{c}, c_{\mathrm{T}}^{c}) \tag{21c}$$

The third phase present in the apparatus is gas. Similarly to several works concerning the modelling of fluidized beds, a plug flow for this phase was assumed. Taking into account the mass transfer from the gas to the liquid phase, Eq. (22) is obtained.

$$S\varepsilon_g \frac{\partial c_T^g}{\partial t} dh = S\varepsilon_g u_b c_T^g - S\varepsilon_g u_b \left(c_T^g + \frac{\partial c_T^g}{\partial h} dh\right) - Sak_{cT}\left(\frac{c_T^g}{K} - c_T^c\right) dh \quad (22)$$

Eq. (22) can be reformulated and simplified to the form:

$$\frac{\partial c_T^g}{\partial t} = -u_b \frac{\partial c_T^g}{\partial h} - \frac{ak_{cT}}{\varepsilon_g}\left(\frac{c_T^g}{K} - c_T^c\right) \quad (23)$$

Eq. (23) is accompanied by conditions (24)

$$c_T^g(h, 0) = c_{T0}^g(h),\ c_T^g(0, t) = c_{Tf}^g(t) \quad (24)$$

The mathematical model of the installation presented in Fig. 2 also includes additional elements such as: a biomass thickening node and a mixing node. Based on the concept of the recirculation ratio ξ and the biomass thickening ratio ϑ, a quantitative description of these elements was introduced to the mathematical model. These parameters are defined as:

$$\xi = \frac{F_{Vr}^c}{F_V^c},\ \vartheta = \frac{c_{Br}}{c_B^c} \quad (25)$$

The definitions can be used to formulate the mass balances of a mixing node and a biomass thickening node. Hence, one obtains

$$c_{Bm}^c = c_B^c \cdot \vartheta \cdot \xi \quad (26)$$

and

$$c_{Am}^c = \xi \cdot c_A^c + (1 - \xi) \cdot c_{Af}^c \quad (27)$$

2.3. Dimensionless form of the mathematical model

Dimensionless state variables are introduced for the purpose of numerical simulations and for simplification of the comparative study of the results obtained for various process conditions.

The model which describes the microbiological process in the biofilm is a moving boundary value problem. For this reason the dimensionless coordinate in the biofilm z is defined as:

$$z = \frac{x - r_0}{L_b(t)} \in [0,\ 1] \quad (28)$$

Due to rescaling the coordinate $x \in [0, L_b]$ to $z \in [0, 1]$ functions of the dimensional variable x which specify the distribution of concentrations in the biofilm are substituted with functions of the dimensionless variable z, according to the following rules:

$$c_A^b(x, t) \to \tilde{c}_A^b(z(t), t),\ c_B^b(x, t) \to \tilde{c}_B^b(z(t), t) \quad (29a)$$

$$\frac{\partial c_T^b(x, t)}{\partial t} = \frac{\partial \tilde{c}_T^b(z, t)}{\partial t} - \frac{\partial \tilde{c}_T^b(z, t)}{\partial z}\frac{z}{L_b}\frac{dL_b}{dt} \quad (29b)$$

$$\frac{\partial c_A^b(x, t)}{\partial x} = \frac{1}{L_b}\frac{\partial \tilde{c}_A^b(z, t)}{\partial z},\ \frac{\partial^2 c_A^b(x, t)}{\partial x^2} = \frac{1}{L_b^2}\frac{\partial^2 \tilde{c}_A^b(z, t)}{\partial z^2} \quad (30a)$$

$$\frac{\partial c_T^b(x, t)}{\partial x} = \frac{1}{L_b}\frac{\partial \tilde{c}_T^b(z, t)}{\partial z},\ \frac{\partial^2 c_T^b(x, t)}{\partial x^2} = \frac{1}{L_b^2}\frac{\partial^2 \tilde{c}_T^b(z, t)}{\partial z^2} \quad (30b)$$

For further analysis dimensionless quantities for the remaining model variables are introduced, i.e. degree of conversion of carbonaceous substrate α, dimensionless biomass concentration in the liquid phase β, dimensionless oxygen concentration in the liquid phase γ, dimensionless concentration of carbonaceous substrate in the biofilm η, and dimensionless concentration of oxygen in the biofilm δ. These quantities are defined as follows:

$$\alpha = \frac{c_{Af}^c - c_A^c}{c_{Af}^c},\ \beta = \frac{c_B^c}{c_{Af}^c},\ \gamma = \frac{c_T^c}{c_{Af}^c} \quad (31a)$$

$$\eta = \frac{\tilde{c}_A^b}{c_A^c},\ \delta = \frac{\tilde{c}_T^b}{c_T^c} \quad (31b)$$

After introducing dimensionless variables, Eqs. (2) and (10), which describe the process in the biofilm, take the form of Eqs. (32).

$$\frac{\partial \eta}{\partial t} = \frac{\eta}{1 - \alpha}\frac{d\alpha}{dt} + \frac{D_{eA}(z)}{L_b^2}\left[\frac{\partial^2 \eta}{\partial z^2} + \left(\frac{1}{D_{eA}(z)}\frac{dD_{eA}(z)}{dz} + \frac{L_b z}{D_{eA}(z)}\frac{dL_b}{dt} + \frac{2L_b}{r_0 + L_b z}\right)\frac{\partial \eta}{\partial z} - \Phi_A^2 \frac{r_A^b(\eta, \delta, z)}{r_A^c}\right] \quad (32a)$$

$$\frac{\partial \delta}{\partial t} = -\frac{\delta}{\gamma}\frac{d\gamma}{dt} + \frac{D_{eT}(z)}{L_b^2}\left[\frac{\partial^2 \delta}{\partial z^2} + \left(\frac{1}{D_{eT}(z)}\frac{dD_{eT}(z)}{dz} + \frac{zL_b}{D_{eT}(z)}\cdot\frac{dL_b}{dt} + \frac{2L_b}{r_0 + L_b z}\right)\frac{\partial \delta}{\partial z} - \Phi_T^2 \frac{r_T^b(\eta, \delta, z)}{r_T^c}\right] \quad (32b)$$

$$\frac{dL_b}{dt} = \frac{L_b}{\tilde{\rho}_b (r_0 + L_b)^2}\int_0^1 (r_0 + zL_b)^2 \cdot r_B^b(z)dz - \frac{k_{det}}{3(r_0 + L_b)^2}\left[(r_0 + L_b)^3 - r_0^3\right] \quad (32c)$$

Thiele moduli in Eqs. 32 are calculated using formulas:

$$\Phi_A^2 = \frac{L_b^2 \cdot r_A^c}{D_{eA}(z) \cdot c_A^c},\ \Phi_T^2 = \frac{L_b^2 \cdot r_T^c}{D_{eT}(z) \cdot c_T^c} \quad (33)$$

Initial and boundary conditions related to Eqs. (32) in a dimensionless form become:

$$\eta(z, 0) = \eta_0(z) \quad (34a)$$

$$\delta(z, 0) = \delta_0(z) \quad (34b)$$

$$L_b(0) = L_{b0} \quad (34c)$$

$$\frac{\partial \eta(0, t)}{\partial z} = 0 \quad (35a)$$

$$\frac{\partial \delta(0, t)}{\partial z} = 0 \quad (35b)$$

$$\frac{\partial \eta(1,\ t)}{\partial z} = \mathrm{Bi}_A\left[1 - \eta(1,\ t)\right] \quad (35c)$$

$$\frac{\partial \delta(1,\ t)}{\partial z} = \mathrm{Bi}_T\left[1 - \delta(1,\ t)\right] \quad (35d)$$

where: $\mathrm{Bi}_A = \frac{k_{sA}L_b}{D_{eA}(1)}$ and $\mathrm{Bi}_T = \frac{k_{sT}L_b}{D_{eT}(1)}$.

Similarly, Eqs. (19) describing the liquid phase are brought to a dimensionless form:

$$\frac{d\alpha}{dt} = -\frac{1}{\tau_0^c}\alpha + r_A^c(\alpha, \beta, \gamma) + \frac{a_s}{(1 - \varepsilon_g)(1 - \zeta)}k_{sA}(1 - \alpha)(1 - \eta(1,\ t)) \quad (36a)$$

$$\frac{d\beta}{dt} = \frac{\vartheta\xi - 1}{\tau_0^c(1 - \xi)}\beta + r_B^c(\alpha, \beta, \gamma) + \frac{1}{c_{Af}}\frac{\zeta}{1 - \zeta}\left(\frac{r_b^3}{r_0^3} - 1\right)\cdot k_{det} x_a \tilde{\rho}_b \quad (36b)$$

$$\frac{d\gamma}{dt} = \frac{1}{\tau_0^c}\left(\gamma_f - \gamma\right) - r_T^c(\alpha,\beta,\gamma) + \frac{m - K\gamma}{\tau_b(1-\varepsilon_g)(1-\zeta)} \left[1 - \exp\left(\frac{-\tau_b a k_{cT}}{K}\right)\right] - \frac{a_s}{(1-\varepsilon_g)(1-\zeta)} k_{sT}\gamma\ \left(1 - \delta(t,\ 1)\right) \quad (36c)$$

where $m = \frac{c_{Tf}^g}{c_{Af}}$, $\tau_b = \frac{H_0}{(1-\varepsilon_g)\cdot u_{0g}}$, $\tau_0^c = \frac{V^c}{F_{Vf}^c}$. Eq. 36 are accompanied by the following initial conditions:

$$\alpha(0) = \alpha_0,\ \beta(0) = \beta_0,\ \gamma(0) = \gamma_0 \quad (37)$$

3. Nonlinear analysis of the steady states in a three-phase fluidized bed bioreactor

The aim of nonlinear analysis of steady states is to determine the parametric dependencies of these states and to assess their local stability. Continuation algorithms are tools for performing such analysis. The application of these algorithms makes it possible to obtain information about steady state multiplicity. Local stability of steady states, turning points, static bifurcation points and Hopf bifurcation points can be found when continuation algorithms are combined with the investigation of local stationary properties. In this paper a continuation algorithm based on local parameterisation was applied for this purpose.

Time derivatives are equal to zero in the steady state, therefore Eqs. (32) and (36) reduce to a system of ordinary differential equations and algebraic equations.

Steady states in the biofilm are described by equations:

$$0 = \frac{d^2\eta}{dz^2} + \left(\frac{1}{D_{eA}(z)}\frac{dD_{eA}(z)}{dz} + \frac{2L_b}{r_0 + L_b z}\right)\frac{d\eta}{dz} - \Phi_A^2 \frac{r_A^b(\eta,\delta,z)}{r_A^c} \quad (38a)$$

$$0 = \frac{d^2\delta}{dz^2} + \left(\frac{1}{D_{eT}(z)}\frac{dD_{eT}(z)}{dz} + \frac{2L_b}{r_0 + L_b z}\right)\frac{d\delta}{dz} - \Phi_T^2 \frac{r_T^b(\eta,\delta,z)}{r_T^c} \quad (38b)$$

Adequate boundary conditions have the form:

$$\frac{d\eta(0)}{dz} = 0 \quad (39a)$$

$$\frac{d\delta(0)}{dz} = 0 \quad (39b)$$

$$\frac{d\eta(1)}{dz} = \mathrm{Bi_A}\left[1 - \eta(1)\right] \quad (39c)$$

$$\frac{d\delta(1)}{dz} = \mathrm{Bi_T}\left[1 - \delta(1)\right] \quad (39d)$$

The biofilm thickness in the steady state is calculated based on Eq. (40).

$$0 = \frac{L_b}{\bar{\rho}_b(r_0 + L_b)^2}\int_0^1 (r_0 + zL_b)^2 \cdot r_B^b(z)dz - \frac{k_{det}}{3(r_0 + L_b)^2}\left[(r_0 + L_b)^3 - r_0^3\right] \quad (40)$$

Processes in the liquid phase can be described with a system of nonlinear algebraic equations

$$0 = -\frac{1}{\tau_0^c}\alpha + r_A^c(\alpha,\beta,\gamma) + \frac{a_s}{(1-\varepsilon_g)(1-\zeta)} k_{sA}(1-\alpha)(1 - \eta(1,\quad t)) \quad (41a)$$

$$0 = \frac{\vartheta\xi - 1}{\tau_0^c\left(1-\xi\right)}\beta + r_B^c(\alpha,\beta,\gamma) + \frac{1}{c_{Af}}\cdot\frac{\zeta}{1-\zeta}\left(\frac{r_b^3}{r_0^3} - 1\right)\cdot k_{det}\bar{\rho}_b x_a \quad (41b)$$

$$0 = \frac{1}{\tau_0^c}\left(\gamma_f - \gamma\right) - r_T^c(\alpha,\beta,\gamma) + \frac{m - K\gamma}{\tau_b(1-\varepsilon_g)(1-\zeta)}\left[1 - \exp\left(\frac{-\tau_b a k_{cT}}{K}\right)\right] - \frac{a_s}{(1-\varepsilon_g)(1-\zeta)} k_{sT}\gamma\ \left(1 - \delta(1,t)\right) \quad (41c)$$

A direct investigation of the stability of steady states can be carried out based on an analysis of dynamic responses to external disturbances. Such an investigation can be realized experimentally on an existing object or by means of numerical simulations of the formulated mathematical model. In this way one obtains time trajectories which characterise the dynamics of the analysed object. However, the stability of a given steady state can be assessed without the solution of a dynamic model, by the evaluation of the eigenvalues of a linearised model.

When the model of the biofilm is initially transformed by finite dimensional approximation, e.g. by means of orthogonal collocation, then the determination of the stability of a steady state reduces to calculation of a certain number of eigenvalues, as for operations in finite dimensional spaces.

Let N be the number of internal collocation points in the biofilm. Then the state vector $Y = [\eta_1, \eta_2, \ldots, \eta_{N+1}, \delta_1, \delta_2, \ldots, \delta_{N+1}, L_b, \alpha, \beta, \gamma] \in \Re^{2(N+1)+4}$ contains whole information about the steady state of the bioreactor. η_i and δ_i are values of functions $\eta(z)$ and $\delta(z)$ at internal collocation points z_i and on the surface of the biofilm, i.e. at $z = 1$.

When the boundary value problem (38) and (39) is approximated using orthogonal collocation, then a system of $2\cdot(N+1)$ algebraic equations is obtained

$$\sum_{i=1}^{N+1} g_{ji}\eta_i + \left(\frac{1}{D_{eA}(z_j)}\frac{dD_{eA}(z_j)}{dz} + \frac{2L_b}{r_0 + L_b z}\right)\cdot\sum_{i=1}^{N+1} m_{ji}\eta_i - \Phi_A^2\frac{r_A^b(\eta_j,\delta_j,z_j)}{r_A^c} = 0 \quad (42a)$$

$$\sum_{i=1}^{N+1} g_{ji}\delta_i + \left(\frac{1}{D_{eT}(z_j)}\frac{dD_{eT}(z_j)}{dz} + \frac{2L_b}{r_0 + L_b z}\right)\cdot\sum_{i=1}^{N+1} m_{ji}\delta_i - \Phi_T^2\frac{r_T^b(\eta_j,\delta_j,z_j)}{r_T^c} = 0 \quad (42b)$$

$$\sum_{i=1}^{N+1} m_{(N+1),i}\eta_i - \mathrm{Bi_A}\left(1 - \eta_{N+1}\right) = 0 \quad (42c)$$

$$\sum_{i=1}^{N+1} m_{(N+1),i}\delta_i - \mathrm{Bi_T}\left(1 - \delta_{N+1}\right) = 0 \quad (42d)$$

In Eq. (42a) and (42b) subscript j changes from 1 to N. Coefficients g_{ji} and m_{ji} are elements of matrices $\boldsymbol{M}$ and $\boldsymbol{G}$, where:

$$\boldsymbol{M} = \boldsymbol{C}\cdot\boldsymbol{Q}^{-1},\quad \boldsymbol{G} = \boldsymbol{D}\cdot\boldsymbol{Q}^{-1} \quad (43)$$

while $\boldsymbol{Q}$ is the matrix of approximating polynomials in collocation nodes, and $\boldsymbol{C}$ is the matrix of the derivatives of these polynomials. Orthogonal polynomials of even orders are applied as approximating polynomials.

Completing the system of Eqs. (42) with the model for the liquid phase (41) and with Eq. (40), which determines the biofilm thickness, one obtains $2\times(N+1)+4$ nonlinear algebraic equations in total.

This system of equations can be written in a vector form as

$$\Psi(Y) = 0,\quad \Psi : \Re^{2(N+1)+4} \to \Re^{2(N+1)+4} \quad (44)$$

where $Y = [\eta_i, \delta_i, L_b, \alpha, \beta, \gamma] \in \Re^{2(N+1)+4}$, $(i = 1, \ldots, N+1)$. A steady state of the analysed bioreactor is determined by a solution of this system of equations.

For the assessment of steady states stability it is sufficient to determine the eigenvalues of Jacobi matrix $\boldsymbol{J}$, where

$$\boldsymbol{J} = \frac{d\Psi}{dY},\ J_{i,j} = \left[\frac{\partial\Psi_i}{\partial Y_j}\right]_{i,j},\ (\mathrm{i,\ j,} = 1, \ldots\ldots 2\times(\mathrm{N}+1)+4) \quad (45)$$

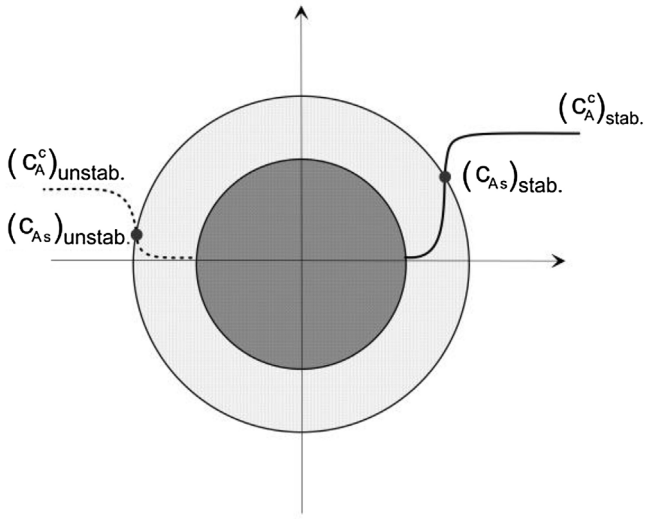

Fig. 3. Graphical illustration of hypothesis 1.

A steady state is stable if all the eigenvalues of the Jacobi matrix (45) have negative real parts [17].

In this paper another method for the determination of the stability of steady states was proposed. The method is based on two hypotheses, which are formulated below.

Hypothesis 1. In a steady state the concentrations of substrates in the liquid phase are related to one and only one set of profiles of concentrations in the biofilm.

The proposed hypothesis 1 is visualized in Fig 3. For clarity, the figure presents profiles of only one substrate, which are related to the stable and unstable steady state of the bioreactor.

Based on hypothesis 1, the next hypothesis was formulated. The way of stability determination of a steady state is given by hypothesis 2.

Hypothesis 2. The eigenvalues of the Jacobi matrix obtained from equations formulated for the liquid phase, global mass balance of biomass in the biofilm, and boundary conditions on a surface of the biofilm determine the character of the linear stability of the steady state.

In other words, the aforementioned Jacobi matrix is formulated for Eq. (39c), Eq. (39d), Eq. (40) and Eq. (41). Hence $Y=[\eta(0), \delta(0), L_b, \alpha, \beta, \gamma] \in \Re^6$ and

$$\Psi(Y)=0, \quad \Psi : \Re^6 \rightarrow \Re^6 \tag{46}$$

The proposed method for the determination of the stability of steady states, which is based on the formulated hypotheses, was numerically verified. For this purpose the method of orthogonal collocation was used. Apart from this, dynamic simulations of the bioreactor were performed.

4. Results and discussion

The results of the nonlinear analysis of steady states and selected results of the dynamic behaviour of the three-phase fluidized bed bioreactor are presented below. The properties of the bioreactor were investigated for two aerobic processes, i.e. for glucose utilization by *Pseudomonas aeruginosa* and phenol biodegradation by *Pseudomonas putida*. The values of kinetic parameters for both microbiological processes are given in Table 2 and Table 3, respectively.

Table 2
Values of kinetic parameters for aerobic utilization of glucose by *Pseudomonas aeruginosa* [18].

k [1/h]	K_A [kg/m^3]	K_T [kg/m^3]	w_{BA} [kg/kg]	w_{BT} [kg/kg]
0.32	$2.032\cdot10^{-2}$	$5.00\cdot10^{-4}$	0.628	0.635

Table 3
Values of kinetic parameters for aerobic biodegradation of phenol by *Pseudomonas putida* [19].

k [1/h]	K_A [kg/m^3]	K_T [kg/m^3]	K_{in} [kg/m^3]	w_{BA} [kg/kg]	w_{BT} [kg/kg]
0.569	$1.8539\cdot10^{-2}$	$4.80\cdot10^{-5}$	$9.9374\cdot10^{-2}$	0.521	0.338

Table 4
Values of parameters p, q (Eq. (47)) and a, b (Eq. (48)) [20].

Bacteria	p	q	a	b
Pseudomonas aeruginosa	0.01125	216.2	16.03	31590
Pseudomonas putida	0.004244	123.2	16.03	31590

Distributions of biofilm density $\rho_b(x)$ and effective diffusion coefficients of substrates in biofilm $D_{ei}(x)$ were determined based on empirical correlations

$$\rho_b(x)=\frac{1}{p+q\cdot(x-r_0)}-\frac{1}{3}\frac{x^3-r_0^3}{x^2}\frac{q}{(p+q(x-r_0))^2} \tag{47}$$

and

$$\frac{D_{ei}(x)}{D_{iw}}=\frac{1}{1+a\cdot\exp(-b(x-r_0))}+\frac{1}{3}\frac{x^3-r_0^3}{x^2}\frac{a\,b\cdot\exp(-b(x-r_0))}{[1+a\cdot\exp(-b(x-r_0))]^2} \tag{48}$$

Parameters of functions defined by Eq. (47) and Eq. (48) are listed in Table 4.

An increase of carbonaceous substrate concentration leads to a limited availability of oxygen in the liquid phase, and eventually oxygen takes the role of a growth-limiting substrate. One can observe a decrease of oxygen concentration in Fig. 4c. In the authors' opinion, the limit values of carbonaceous substrate concentration, for which oxygen becomes the limiting substrate, corresponds to the maximum values of the biofilm thickness in Fig. 4d. Above those values of the carbonaceous substrate concentration, the rate of the microbiological process is limited by oxygen dissolved in the liquid phase. Finally, this leads to a decrease of the degree of conversion α and lower values of biofilm thickness L_b, which can be observed in Fig. 4a and d, respectively.

Similar calculations were performed for phenol biodegradation to assess the influence of substrate inhibition. Fig. 5 reports stationary characteristics of the bioreactor for two values of mean residence time of the liquid phase.

An occurrence of a minimum of the value of oxygen concentration can be observed in Fig. 5c independently of mean residence time of the liquid phase in an installation. This extreme was not observed for the process without substrate inhibition. The concentration of carbonaceous substrate which corresponds to the minimum is simultaneously a limit value of a sufficiently high degree of conversion α. Higher values of phenol concentration c_{Af} result in lower values of degree of conversion. At the same, despite thicker biofilms, the concentration of biomass in the liquid phase decreases, which probably corresponds to the phenomenon of substrate inhibition in this phase. The maximal value of biofilm thickness observed in Fig. 5d probably corresponds to the substrate concentration for which inhibition starts to occur in the biofilm. Hence, there are two limit values of phenol concentration in the liquid phase which reveal the substrate inhibition phenomenon. One of these values, the lower one, is related to the liquid phase, and the second one to the biofilm. A shift towards higher concentrations of phenol in the case of the biofilm is probably caused by

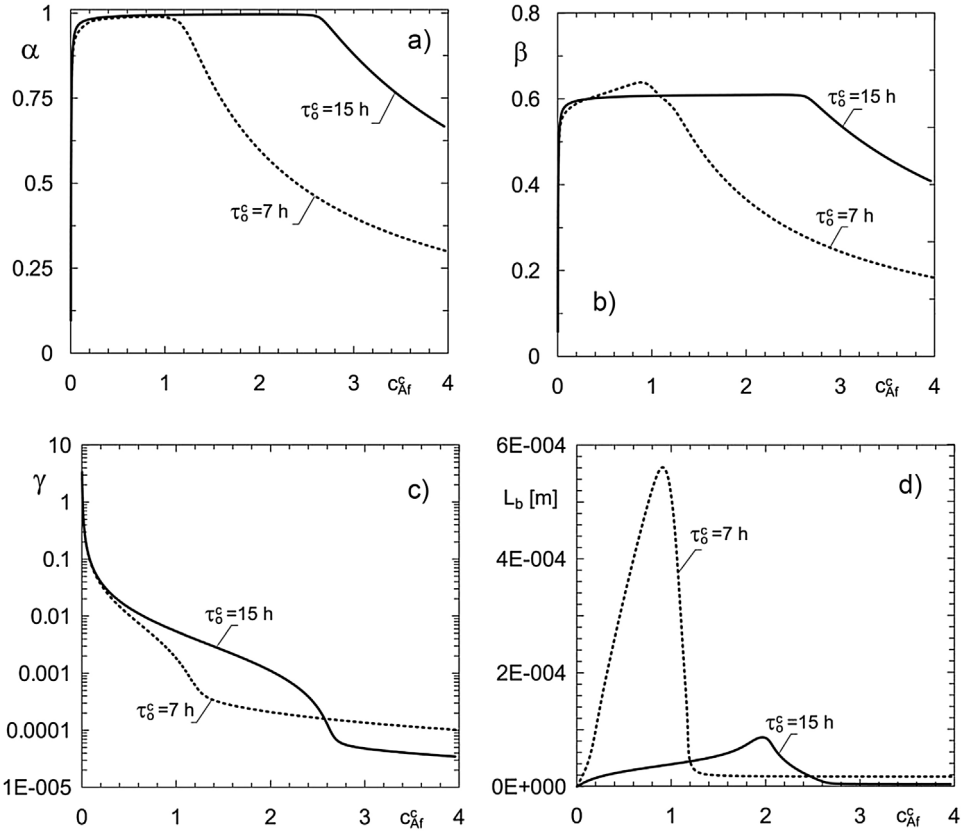

Fig. 4. Steady state branches of three-phase fluidized bed bioreactor obtained for glucose utilization ($x = 0.2$; $\vartheta = 0.9$; $\rho_0 = 2300\,kg/m^3$).

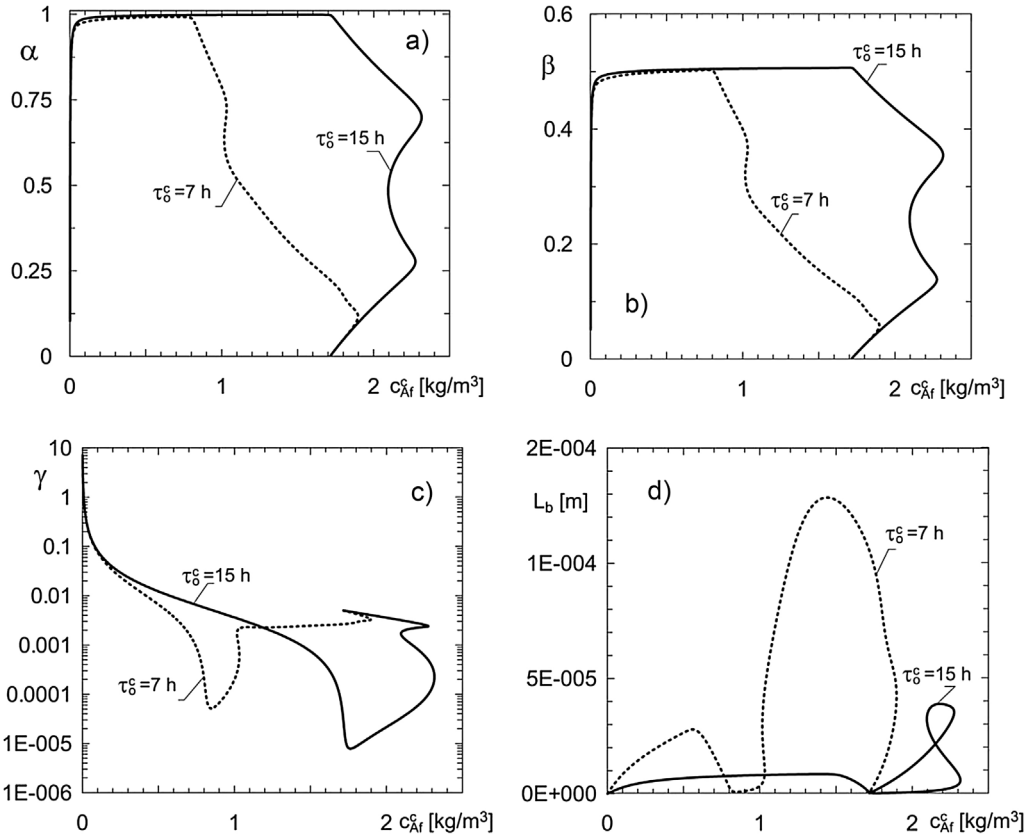

Fig. 5. Steady state branches of three-phase fluidized bed bioreactor for phenol biodegradation ($x = 0.2$; $\vartheta = 0.9$; $\rho_0 = 2300\,kg/m^3$).

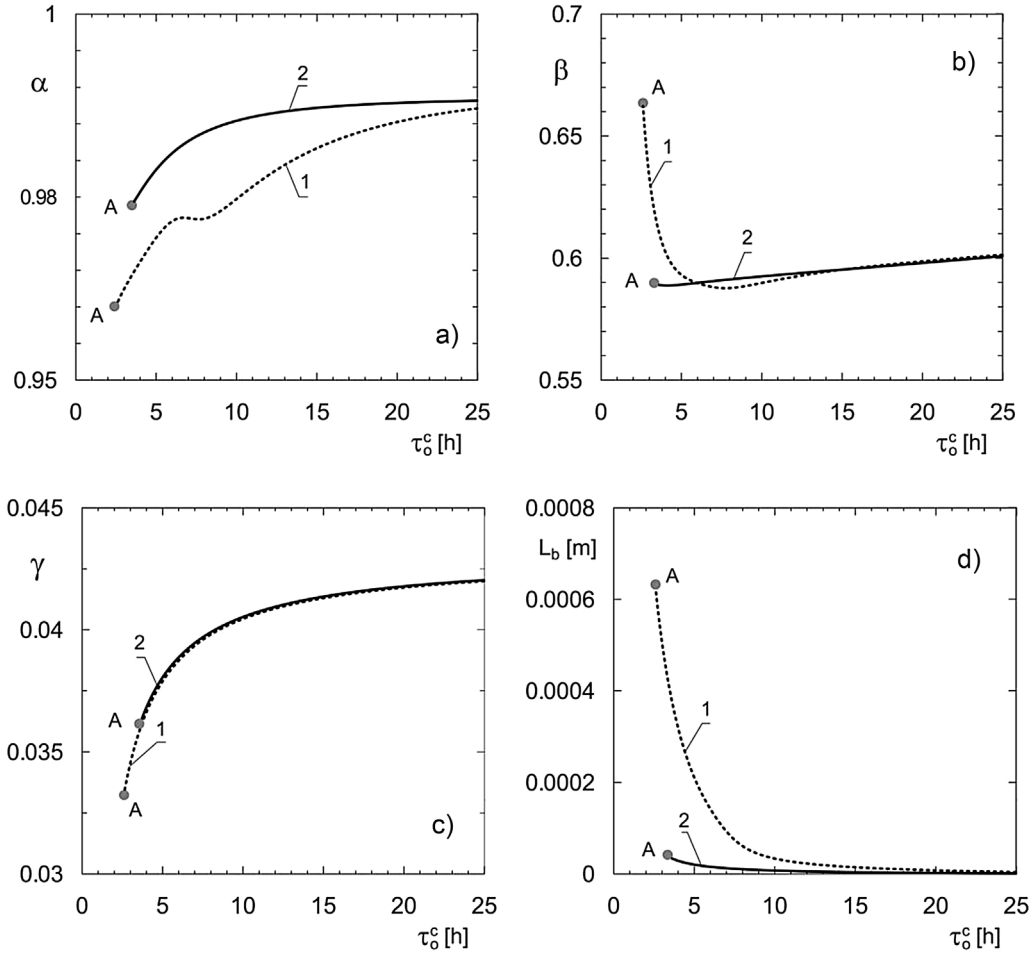

Fig. 6. Steady state branches of three-phase fluidized bed bioreactor for two values of ζ (glucose utilization; at points A the condition $u_{0c} = u_t$ is fulfilled) ($c_{Af} = 0.2$ kg/m^3; $x = 0.2$; $\vartheta = 0.9$; $\rho_0 = 1400$ kg/m^3) 1- $\zeta = 0.01$; 2- $\zeta = 0.05$.

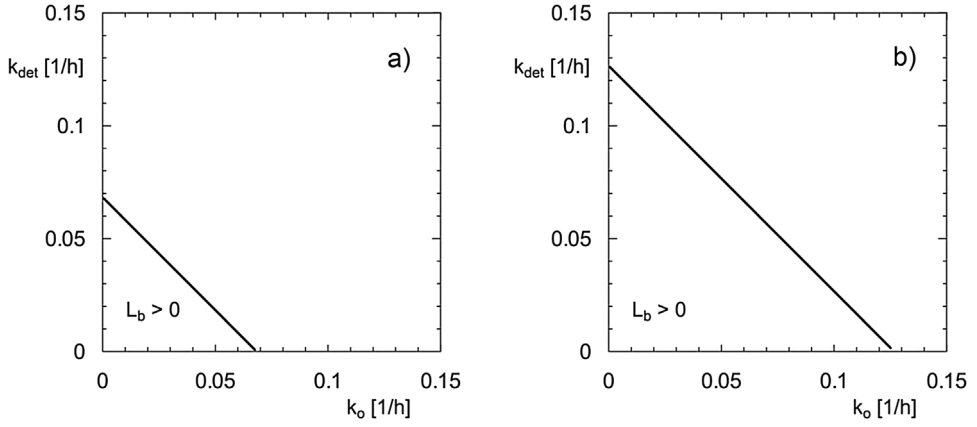

Fig. 7. The region of biofilm existence on inert carrier particles of diameter $d_0 = 7 \cdot 10^{-4}$ m in the three-phase fluidized bed bioreactor depending on the decay rate coefficient of microorganisms k_o and the biofilm detachment rate coefficient k_{det} (glucose utilization) a) $x = 0.2$; b) $x = 0.9$ ($c_{Af} = 0.2$ kg/m^3; $\tau_o^c = 15$ h; $\vartheta = 0.9$; $u_{0g} = 0.005$ m/s; $\zeta = 0.01$; $\rho_0 = 2300$ kg/m^3).

concentration distributions inside the biofilm. Neither such results nor process interpretation have been published previously in the literature.

When phenol concentration is high enough, inhibition occurs both in the liquid phase and in the biofilm. In such a case, despite the availability of both substrates, a low degree of conversion α, biomass concentration β and biofilm thickness are observed.

Based on results presented in Fig. 6 it is possible to assess the influence of the mean residence time of the liquid phase on state variables in the three-phase fluidized bed bioreactor. Intuitively, an increase of this parameter results in an increase in the degree of conversion of the carbonaceous substrate. The rise of this variable is significant only in the range of small values of mean residence time. A further increase of this parameter causes slight changes of

the degree of conversion α. This information is useful for designers and technologists.

The analysis of steady state branches obtained for two values of a fraction of carrier particles $\zeta = 0.01$ and $\zeta = 0.05$ indicates the moderate influence of this quantity on state variables in the case of sufficiently high values of mean residence time. The situation changes when the value of mean residence time is low. Then, the higher fraction of particles results in higher degrees of conversion of the carbonaceous substrate.

Interpretation of the diagram shown in Fig. 6d allows us to explain the reasons for the above-mentioned observation. The use of smaller fraction of solid particles is associated with a decrease in their number. Hence, the surface covered by the biofilm is smaller, and so is the surface of interphase mass transfer. The decrease of this surface results in a higher biofilm thickness. Then, due to biomass transfer from the biofilm to the liquid phase, the increase of the biofilm thickness results in a higher concentration of biomass in the liquid phase (shown in Fig. 6b).

The limitation, which results from the hydrodynamics of the fluidized bed, is taken into account in the results presented in Fig. 6. Points marked with the letter A correspond to conditions when the velocity of the liquid is equal to the terminal velocity of bioparticles.

The biofilm thickness is significantly affected by the values of the decay rate coefficient of microorganism k_o and the biofilm detachment rate coefficient k_{det}. Hence, it was decided to perform simulations aiming at the determination of the conditions of biofilm existence on solid carriers. To this end, biofilm thickness equal to zero was assumed, and then for a fixed value of k_o a value of k_{det} was determined. Obtained relations are presented in Fig. 7.

It was proved that both parameters have a linear influence on the boundary of biofilm existence. For a fixed value of the decay rate coefficient of microorganisms there exists such a limit value of the biofilm detachment rate coefficient above which the biofilm disappears. It is an important property, which has not previously been mentioned in the literature. This property can be used, e.g. for the intentional removal of biofilm by means of biocides, or in the opposite manner to prevent its removal.

As expected, a higher value of k_o corresponds to a lower value of k_{det}. The region of biofilm existence is under the border line. It is worth noticing that an increase of recirculation ratio ξ leads to an increase of the biofilm existence region, which is shown in Fig. 7b. Such a phenomenon is a result of the partial washout of biomass from the liquid phase, and a consequent increase of substrate availability for microorganisms in the biofilm. Higher values of substrate concentrations lead to a higher rate of biomass growth in the biofilm, and this is a reason for the broadening of the existence area of the biofilm.

Hereafter, representative results of the stability analysis are presented. The stability was analysed according to the two hypotheses formulated in this paper. Furthermore, a comparison of the stability assessment based on these hypotheses and on the orthogonal collocation method was conducted. It was observed that the results of the stability analysis are identical and independent of the method employed. On this basis one can come to a conclusion with cognitive and practical importance. The proposed, simpler method for the stability assessment of steady states in a three-phase fluidized bed bioreactors is well-founded, and it is not necessary to use any additional tool, such as orthogonal collocation or another method for the finite dimensional approximation of the biofilm model.

Fig. 8a–d presents an alternate character of the stability of steady states for the region of multiple steady states. Based on the stability analysis, it was confirmed that the process giving a high degree of conversion can be carried out even when biofilm thickness is low. Simultaneously, the existence of steady states corresponding to thick biofilms and rather low degrees of conversion α was demonstrated. This information is important during the operation of such bioreactors.

A similar analysis was conducted for a lower concentration of carbonaceous substrate for which steady state multiplicity should not occur. Results are shown in Fig. 8e–h. For a lower concentration of the carbonaceous substrate, turning points do not occur on steady state branches. Hence, there are single steady states in a whole range of values of mean residence time. The analysis of their stability shows the existence of a range of unstable steady states which occur between Hopf bifurcation points. Sustained oscillations of the state variables originate in these characteristic points.

It is necessary to solve the system of differential Eqs. (32) with boundary conditions (34), (35) and the system of Eqs. (36) with conditions (37) to characterize the quantitative dynamic properties of the bioreactor. The system of partial differential equation was solved using the method of lines [21]. Finally, we obtained a system of ordinary differential equations, which was integrated by means of Gear's method [22]. Except this algorithm, all required programs have been created by the authors in Fortran language.

Time trajectories of state variables, i.e. $\alpha(t)$, $\beta(t)$, $\gamma(t)$ and $L_b(t)$ are presented in Fig. 9. The set of process parameters used in simulations corresponds to point B in Fig. 8e–h. Presented trajectories are dynamic responses of the system to two disturbances with different amplitudes. The first one is rather small and corresponds to initial conditions equal to 0.9 of state variables values in the steady state. The response to this disturbance is marked with line "1". Line "2"corresponds to time trajectories obtained as a response to a large disturbance, i.e. initial conditions are 0.2 of values of state variables in the steady state.

The degree of conversion α and oxygen concentration in the liquid phase γ return to the neighbourhood of the steady state quite quickly after the small disturbance (curves "1"). The return of biofilm thickness and biomass concentration to the steady state lasts significantly longer. In the case of these variables, even after a small disturbance, reaching the steady state lasts about 100 h.

When the bioreactor is affected by large disturbances of state variables, then a longer time is necessary for return to a sufficiently close neighbourhood of the steady state. Despite an almost ten times higher disturbance, the degree of conversion and oxygen concentration in the liquid phase reach the steady state several times faster than the biofilm thickness and biomass concentration in the liquid phase.

The main conclusion from the analysis of time trajectories presented in Fig. 9 is related to different change rates of individual state variables. The rate of change of the biofilm thickness decides the resultant dynamics of the bioreactor.

Fig. 10 reports results concerning the dynamic behaviour of the three-phase fluidized bed bioreactor around the unstable steady state, marked with point "C" in Fig. 8e–h, and lying in a region of unique steady states. The stability assessment shows that this steady state is unstable, and what is more, it is placed between two Hopf bifurcation points. It is known from nonlinear dynamics theory that sustained oscillations of state variables should exist in the neighbourhood of such a steady state. The time trajectories presented in Fig. 10 show such oscillations characterized by a constant value of amplitude and period. The oscillation period lasts about 190 h. Results concerning oscillations of state variables in three-phase fluidized bed bioreactors, including oscillations of biofilm thickness, have not been previously published.

5. Conclusions

The innovative mathematical model of three-phase fluidized bed bioreactors was formulated in this paper. The model takes into account several important elements which are usually not consid-

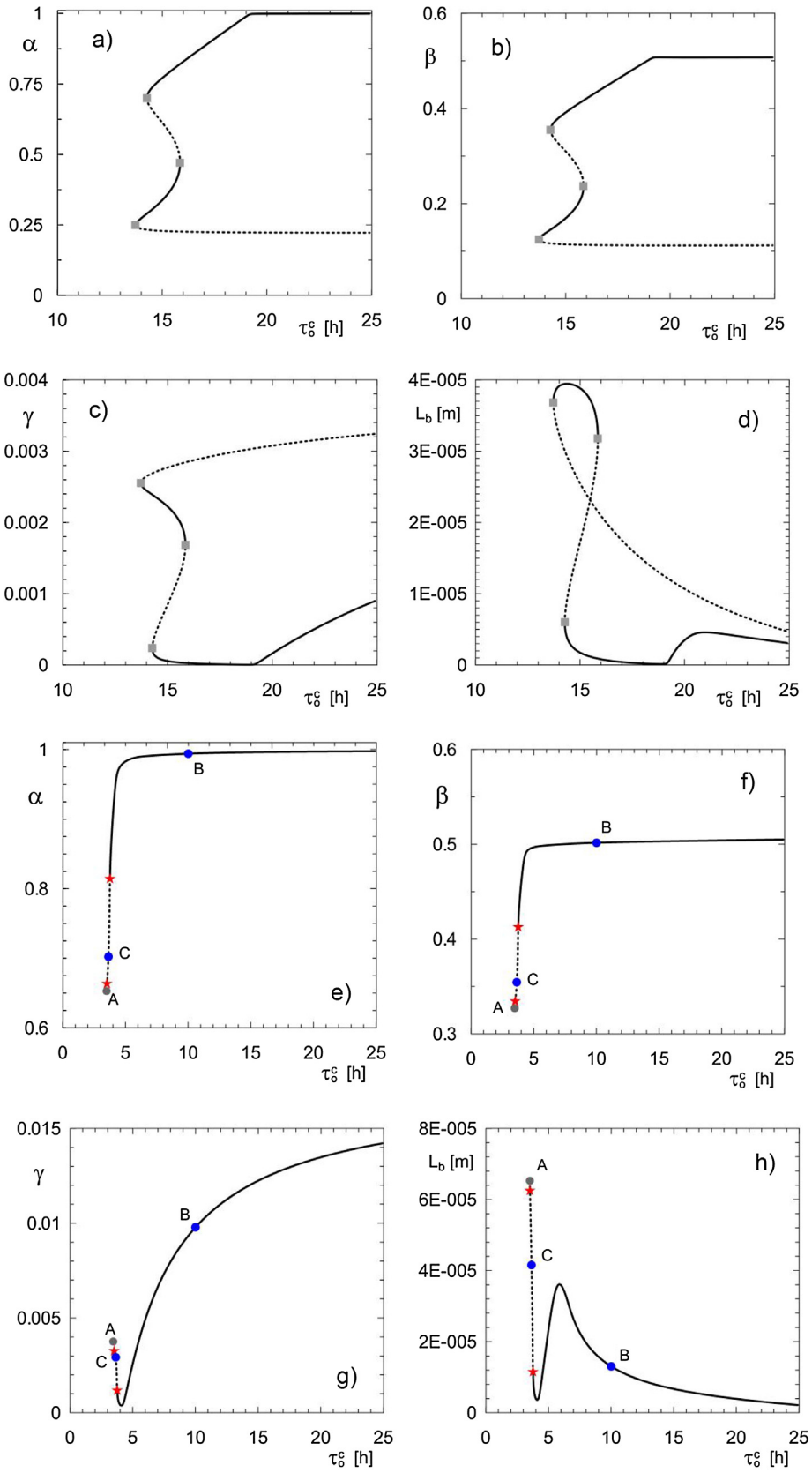

Fig. 8. Linear stability of a chosen branch of steady states in a three-phase fluidized bed bioreactor for phenol biodegradation (■ – turning points; * – Hopf bifurcation points) (at point A condition $u_{0c} = u_t$ is fulfilled) (a–d – $c_{Af} = 2.2\ kg/m^3$) e–h – $c_{Af} = 0.5\ kg/m^3$); ($x = 0.5$; $\vartheta = 0.9$; $\rho_0 = 2300\ kg/m^3$).

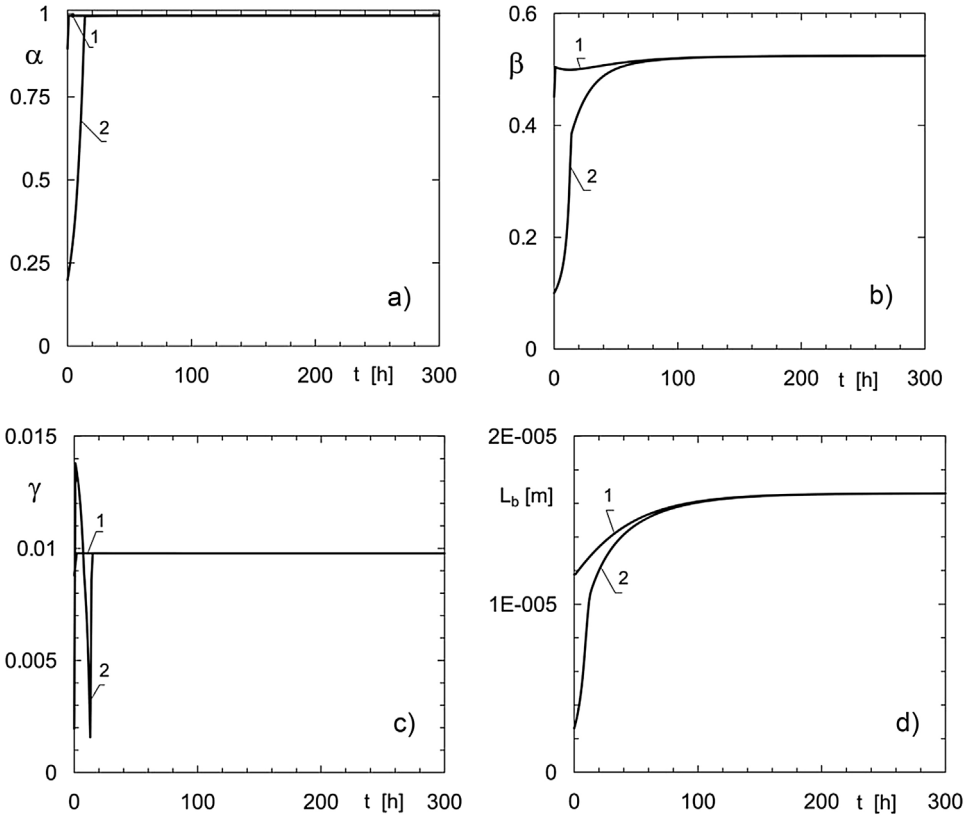

Fig. 9. Time trajectories of state variables, which verifies the stability of a chosen steady state marked with point B in Fig. 8e–h in a three-phase fluidized bed bioreactor. 1- $x_i(0) = 0, 9x_i^*$; 2- $x_i(0) = 0, 2x_i^*$; x_i^*- value i-th state variable at the steady state ($d_0 = 7{\cdot}10^{-4}$ m; $c_{Af} = 0.5$ kg/m^3; $\tau_o^c = 10$ h; $x = 0.2$; $\vartheta = 0.9$; $\rho_0 = 2300$ kg/m^3).

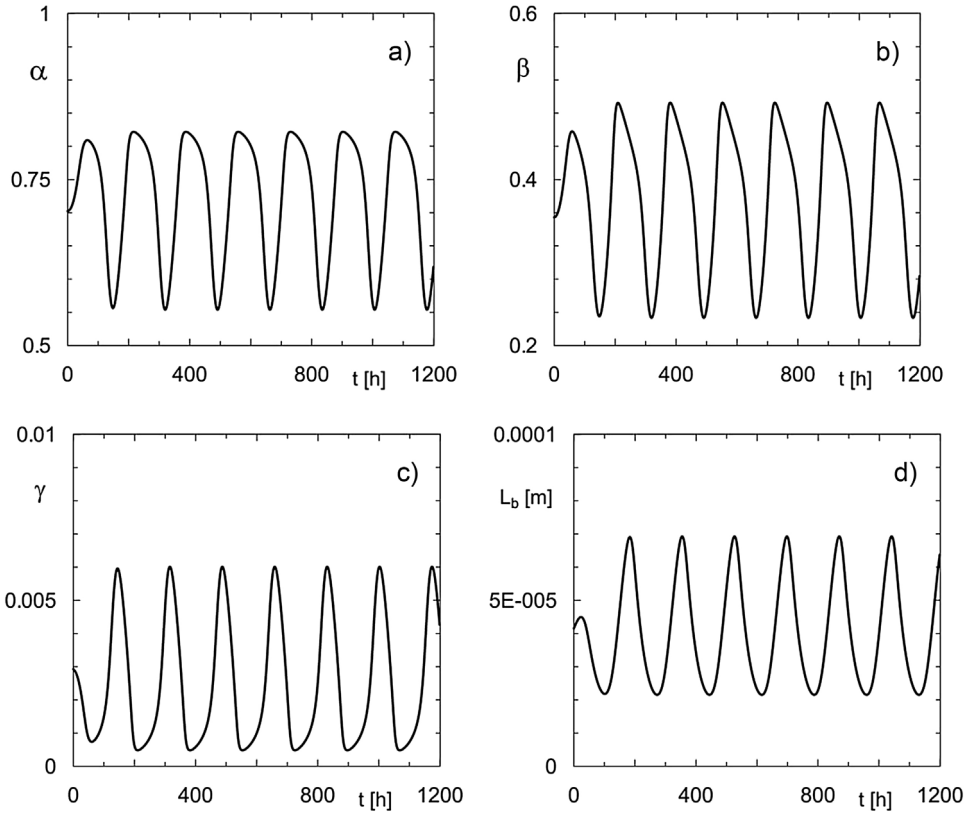

Fig. 10. Time trajectories of state variables in the three-phase fluidized bed bioreactor around the steady state marked as "C" in Fig. 8e–h. ($d_0 = 7{\cdot}10^{-4}$ m; $c_{Af} = 0.5$ kg/m^3; $\tau_o^c = 3.65$ h; $x = 0.2$; $\vartheta = 0.9$; $\rho_0 = 2300$ kg/m^3).

ered, i.e. partial recirculation of the biomass and its thickening, external mass transfer resistance and distributions of density of the biofilm, as well as distributions of effective diffusion coefficients in the biofilm.

A method for the determination of steady states of the investigated apparatus was also proposed. Moreover, the way of performing dynamic simulations based on the method of lines was also proposed. Systematic research on the steady state structure was conducted, taking into account the effect of the kinetic model of microbial growth. Regions of multiple steady states and Hopf bifurcation points in the region of single steady states were found.

A detailed process interpretation of steady state branches was performed for two aerobic processes. Based on the presented stationary characteristics it is stated that in three-phase fluidized bed bioreactors two limit values of substrate concentration in the inlet stream can exist, which are related with the inhibition phenomenon in the liquid phase and in the biofilm.

The stability of steady states was assessed using three methods, i.e. dynamic analysis, a finite dimensional approximation, and the proposed simplified method. The authors' simplified method is based on two hypotheses formulated in this paper, from which one can deduce that for the stability assessment it is sufficient to investigate the eigenvalues of a system of equations describing the dynamics of the liquid phase, biofilm thickness, and boundary conditions at the biofilm-liquid interphase. As a result, when the simplified method is applied, it is not necessary to use advanced numerical methods for the discretisation of partial differential equations along the spatial variable in the biofilm. It was shown that the stability assessment is independent from all the three methods tested.

The existence of sustained oscillations of state variables was discovered through dynamic analysis of the bioreactor. It was observed that individual state variables are characterised by different time constants, and the overall dynamics of the bioreactor depends on biofilm thickness dynamics.

The presented results have both cognitive and practical significance. Similar results for fluidized bed biofilm reactors have not been published previously, and information on unstable steady states in the region of single steady states could be of key importance for the start-up of apparatus and process operation. The simplified method of stability assessment can be applied for process calculations and for the design of three-phase fluidized bed bioreactors.

References

[1] K.A. Onysko, C.W. Robinson, H.M. Budman, Improved modelling of the unsteady-state behaviour of an immobilized-cell, fluidized-bed bioreactor for phenol biodegradation, Can. J. Chem. Eng. 80 (2002) 239–252.
[2] W.-T. Tang, L.-S. Fan, Steady state phenol degradation in a draft-tube, gas-liquid-solid fluidized-bed bioreactor, AIChE J. 33 (1987) 239–249.
[3] W.-T. Tang, K. Wisecarver, L.-S. Fan, Dynamics of a draft tube gas-liquid-solid fluidized bed bioreactor for phenol degradation, Chem. Eng. Sci. 42 (1987) 2123–2134.
[4] K.D. Wisecarver, L.S. Fan, Biological phenol degradation in a gas-liquid-solid fluidized bed reactor, Biotechnol. Bioeng. 33 (1989) 1029–1038.
[5] R.M. Worden, T.L. Donaldson, Dynamics of a biological fixed film for phenol degradation in a fluidized-bed bioreactor, Biotechnol. Bioeng. 30 (1987) 398–412.
[6] I.J. Dunn, H. Tanaka, S. Uzman, M. Denac, Biofilm fluidized-Bed reactors and their application to waste water nitrification, Ann. N. Y. Acad. Sci. 413 (1983) 168–183.
[7] Y. Park, M.E. Davis, D.A. Wallis, Analysis of a continuous aerobic, fixed-film bioreactor. II. Dynamic behavior, Biotechnol. Bioeng. 26 (1984) 468–476.
[8] Y. Park, M.E. Davis, D.A. Wallis, Analysis of a continuous aerobic, fixed-film bioreactor. I. Steady-state behavior, Biotechnol. Bioeng. 26 (1984) 457–467.
[9] M. Sarrà, C. Casas, F. Gòdia, Continuous production of a hybrid antibiotic by Streptomyces lividans TK21 pellets in a three-phase fluidized-bed bioreactor, Biotechnol. Bioeng. 53 (1997) 601–610.
[10] Y.L. Huang, C.H. Shu, S.T. Yang, Kinetics and modeling of GM-CSF production by recombinant yeast in a three-phase fluidized bed bioreactor, Biotechnol. Bioeng. 53 (1997) 470–477.
[11] K. Schugerl, Three-phase-biofluidization – application of three-phase fluidization in the biotechnology – a review, Chem. Eng. Sci. 52 (1997) 3661–3668.
[12] H.T. Chang, B.E. Rittmann, Mathematical modeling of biofilm on activated carbon, Environ. Sci. Technol. 21 (1987) 273–280.
[13] M.E. Russo, P.L. Maffettone, A. Marzocchella, P. Salatino, Bifurcational and dynamical analysis of a continuous biofilm reactor, J. Biotechnol. 135 (2008) 295–303.
[14] G. Olivieri, M.E. Russo, A. Marzocchella, P. Salatino, Modeling of an aerobic biofilm reactor with double-limiting substrate kinetics: bifurcational and dynamical analysis, Biotechnol. Prog. 27 (2011) 1599–1613.
[15] A.G. Livingston, Biodegradation of 3,4-dichloroaniline in a fluidized bed bioreactor and a steady-state biofilm Kinetic model, Biotechnol. Bioeng. 38 (1991) 260–272.
[16] H. Beyenal, A. Tanyolaç, The effects of biofilm characteristics on the external mass transfer coefficient in a differential fluidized bed biofilm reactor, Biochem. Eng. J. 1 (1998) 53–61.
[17] R. Seydel, Practical bifurcation and stability analysis, Springer, 2009.
[18] H. Beyenal, S.N. Chen, Z. Lewandowski, The double substrate growth kinetics of Pseudomonas aeruginosa, Enzyme Microb. Technol. 32 (2003) 92–98.
[19] S. Seker, H. Beyenal, B. Salih, A. Tanyolac, Multi-substrate growth kinetics of Pseudomonas putida for phenol removal, Appl. Microbiol. Biotechnol. 47 (1997) 610–614.
[20] B. Tabis, R. Siudzinska, The assessment of density and diffusivity distributions in a biofilm immobilized on fine particles, Przem. Chem. 84 (2005) 250–253.
[21] A. Zafarullah, Application of the method of lines to parabolic partial differential equations with error estimates, JACM 17 (1970) 294–302.
[22] C.W. Gear, Algorithm 407: DIFSUB for solution of ordinary differential equations [D2], Commun. ACM 14 (1971) 185–190.